DOI 10.1007/s10593-016-1810-1

Chemistry of Heterocyclic Compounds **2015**, *51*(11/12), 997–1007

Experimental and quantum-chemical study of nucleophilic substitution mechanism in berberine

Oleg N. Burov[1]*, Mikhail E. Kletskii[1], Nikita S. Fedik[1], Sergey V. Kurbatov[1], Anton V. Lisovin[1]

[1] *Southern Federal University, 7 Zorge St., Rostov-on-Don 344090, Russia; e-mail: bboleg@gmail.com*

Translated from Khimiya Geterotsiklicheskikh Soedinenii, 2015, *51*(11/12), 997–1007

Submitted November 4, 2015
Accepted December 14, 2015

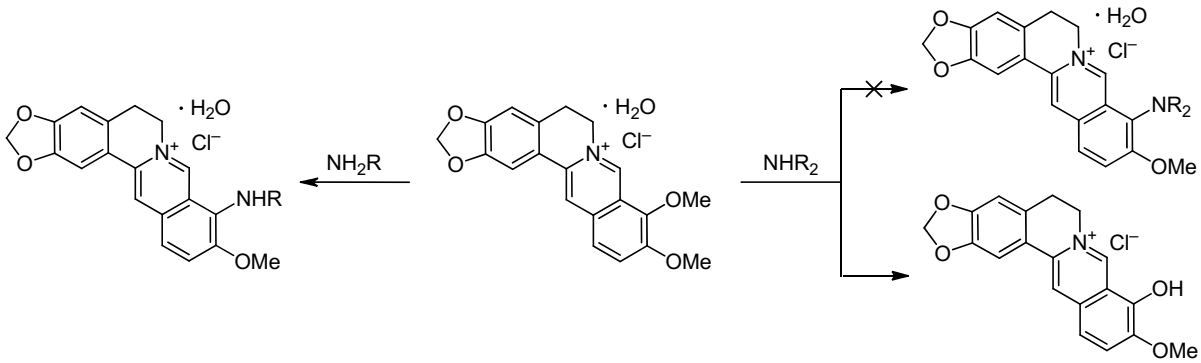

Principal differences in the interaction mechanisms of alkaloid berberine with primary and secondary amines were investigated experimentally and by quantum-chemical calculations according to density functional theory (DFT/B3LYP) with 6-31G** basis set. The nucleophilic substitution of 9-metoxy group with primary amine was shown to proceed through a stage of σ-complex formation and led to 9-alkylamino derivatives of berberine. Analogous substitution with a secondary amine did not occur due to unfavorable thermodynamic parameters. The secondary amine participated in this reaction not as the attacking nucleophile, but rather as a bifunctional catalyst of berberine hydrolysis to berberrubine. The driving force for all these processes was the stabilization of products by hydrogen bonding. Based on the obtained results, we developed a new effective method for the preparation of berberrubine, one of the key intermediates in synthetic transformations of berberine. New 9-monoalkylamino derivatives of berberine containing indole moieties were synthesized.

Keywords: berberine, berberrubine, alkylamination, catalytic hydrolysis, DFT calculations.

The alkaloid berberine (berberine chloride) exhibits a unique set of medicinally important properties, as recently described in several review articles.[1–6] For example, it reduces bleeding, shows antispasmodic, antigastric, hypolipidemic, antiarrhythmic, and hypotensive effects. The antimicrobial, antitumor, and antileucosis activity of berberine have been experimentally proven. Berberine is also used in medicinal chemistry as a fairly reactive molecular scaffold, containing at least four diversification sites: C-8, C-9, C-13, and N-7.

The main methods for the preparation of berberine derivatives have been described in a review.[7] Of special interest among these are the 9-*O*- and 9-*N*-alkyl derivatives of berberine, for two reasons. Firstly, these compounds show valuable medicinal properties by reducing the symptoms of Alzheimer's disease and senile dementia, and increasing acetylcholine concentration by inhibition of acetylcholinesterase (AChE).[8,9] Secondly, these compounds can take part in π–π-interactions with DNA G-quadruplex structures.[10–12] The introduction of an amino group at position 9 of berberine molecule resulted in a strong interaction with the telomeric DNA G-quadruplexes and an inhibiting effect on telomerase, possibly due to an increased electrostatic interaction between the terminal amino group of the side chain and the phosphate backbone in the G-quadruplex of DNA.[13]

It has been reported[12] that 9-*N*-substituted berberine derivatives show a pronounced inhibitory effect on the transcription of c-Myc gene in tumor cells and enhanced cytotoxicity, compared to berberine.[11] Thus, there is a significant interest in the field of medicinal chemistry towards the development of methods for functionalization

Scheme 1

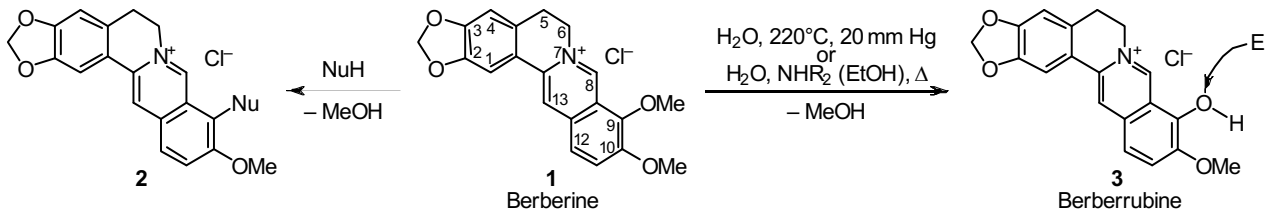

of berberine at position 9, for example, by introducing amino groups.

Two methods are commonly used for the functionalization of berberine (Scheme 1): nucleophilic substitution of the 9-metoxy group in berberine (**1**), forming products with the general structure **2**, and the interaction of berberrubine (**3**) (OH-derivative of berberine) with electrophiles.

Primary aliphatic amines are typically used as nucleophiles (NuH), while alkyl halides[14] and halides[15] serve as electrophiles. It should be noted that, according to Chemical Abstracts, 9-dialkylamino derivatives of berberine have never been described, while the greater nucleophilicity of secondary amines compared to primary amines should enhance their reactivity in the substitution of 9-metoxy group.

The goal of this study was to determine the reasons for such an unusual selectivity of berberine with regard to the structure of amine. For this, we at first performed a comparative experimental and quantum-chemical study (DFT calculations with B3LYP/6-31G** basis set) of berberine reaction with primary and secondary amines.

1. The reaction of berberine with methylamine

All the previously proposed methods for the synthesis of 9-amino derivatives of berberine gave the target products in 25 to 60% yields (the majority of compounds were obtained in 40–45% yields). The main procedure used for these syntheses was refluxing of berberine with the respective amine in absolute alcohol for many hours.[9,11,16] Procedure for the first developed by us involves the reaction of berberine with amines in the absence of solvent, giving 9-aminoberberines **4a**–**d** in higher 50 to 60% yields (Scheme 2).

The interaction of berberine with secondary amines under analogous conditions did not lead to the formation of 9-dialkylamino derivatives. In order to explain this result, we calculated the minimum energy pathway (MEP) of nucleophilic attack by methylamine molecule on berberine (**1**). According to the obtained data, this process eventually leads to the formation of salt **4e**, which consists of methylamine derivative in cation form and a chloride anion (Scheme 2).

We found three stable topomers for this ion pair, the most stable of which (topomer **4e**) contained a Cl^- ion coordinated with a proton of the amino group. It was more stable by 6.6 kcal/mol than the topomer **4e'**, in which the methyl group was oriented towards the Cl^- ion, and more stable by 17.5 kcal/mol than the topomer **4e''**, in which the chloride ion was coordinated with the H-13 proton (Fig. 1).

For the three systems **4e**, we performed a topological analysis of electron density distribution function according to the "atoms in molecules" (AIM) model.[17] The obtained data indicate that there were two attractive interactions in the most stable topomer **4e**. We identified critical points (3,–1) characteristic for the shortened $Cl^-\cdots H–N$ contact [$\rho(\boldsymbol{r}_c) = 1.1\cdot10^{-2}$, $\nabla^2\rho(\boldsymbol{r}_c) = 3.1\cdot10^{-2}$] and a weak attractive $Cl^-\cdots H(8)$ interaction of similar magnitude [$\rho(\boldsymbol{r}_c) = 1.1\cdot10^{-2}$, $\nabla^2\rho(\boldsymbol{r}_c) = 3.2\cdot10^{-2}$]* (Fig. 1). This type of double coordination stabilized the system by 6.6 kcal/mol (taking into account the correction for zero-point energy (ZPE)). At the same time, the topomeric forms **4e'** and **4e''** were characterized by only one attractive interaction of chloride ion with the berberine molecule (Fig. 1). More detailed data are available in Table S1 in the Supplementary information file.

The nucleophilic attack by methylamine on the berberine molecule begins with the barrierless formation of aggregate **5** of these two molecules, which is more stable by 5.3 kcal/mol than the isolated reactants. The reaction further proceeds through the transition states **TS 1** and **TS 2**, forming the hydrogen bond-stabilized intermediate **6**, with the sequence of low-barrier processes resulting in the complex **7**, which is stabilized by a chain of two hydrogen bonds. In general, this entire process is thermodynamically favorable (Scheme 3, Fig. 2; the most important stationary points on MEP are given in Table S2 in the Supplementary information file).

* $\rho(\boldsymbol{r}_c)$ – electron density; $\nabla^2\rho(\boldsymbol{r}_c)$ – the Laplacian of electron density.

Scheme 2

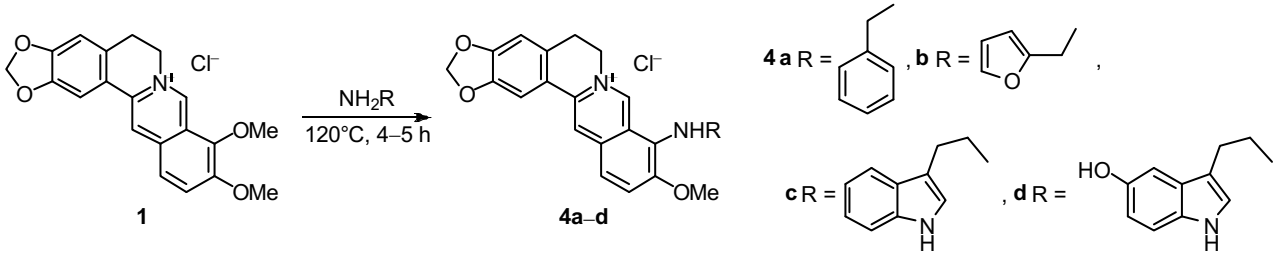

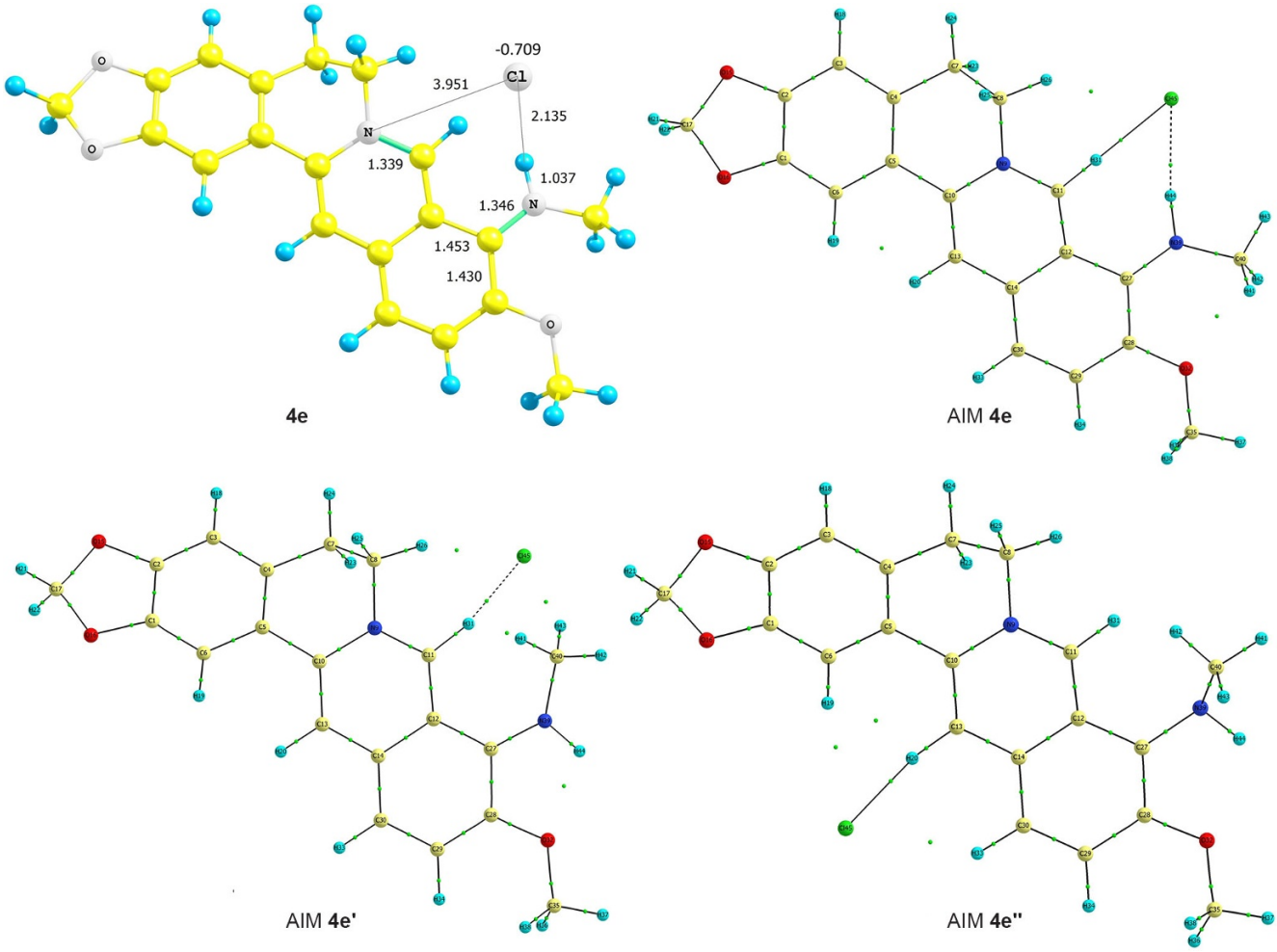

Figure 1. The calculated interatomic distances (Å) in 9-*N*-methylberberine (**4e**). The attractive forces in the three topomers of compound **4e** are also shown.

At the same time, in the case of dimethylamine, the formation of 9-*N*,*N*-dimethylberberine (**4f**) in a bimolecular nucleophilic process is thermodynamically unfavorable, since the sum of energy of molecule **4f** and methanol at infinite separation was higher by 1.4 kcal/mol than the energy of reactants (Scheme 4, Table S3 in the Supplementary informetion file). The chloride ion in system **4f** was shifted to a peripheral location and practically did not stabilize the salt by additional attractive interactions, as was found in the case of primary amine in compound **4e** (Fig. 3, the results of AIM calculations are presented in Figure S10 of the Supplementary information file).

Scheme 3

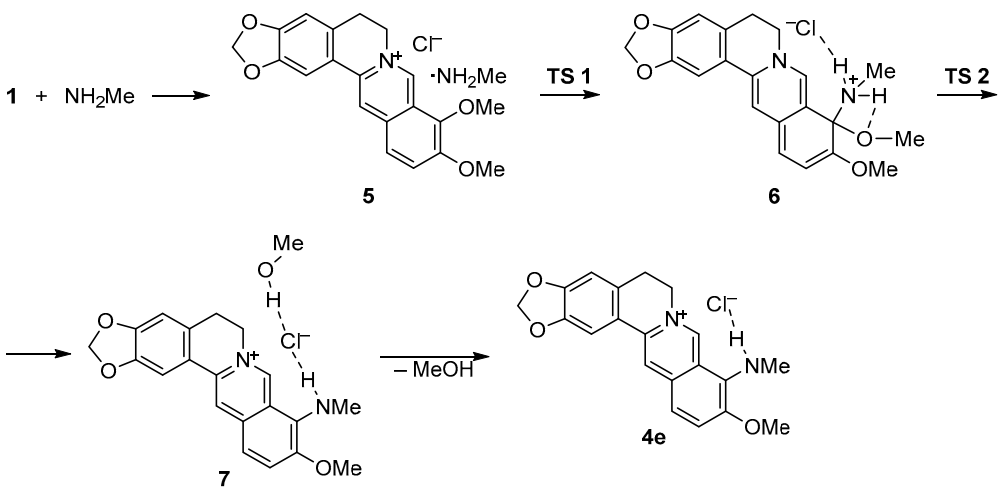

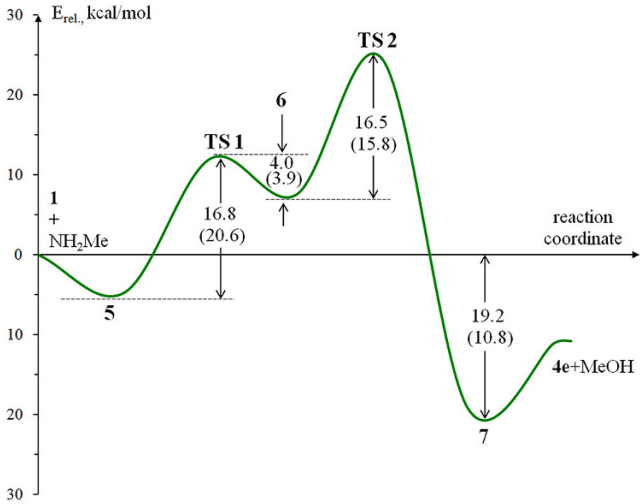

Figure 2. MEP of berberine amination with methylamine. The relative energy values are given taking into account the corrections for ZPE. The relative Gibbs free energy values are given in parentheses. The total energy of isolated reactants is assumed as reference (see Scheme 3 and Table S2 in the Supplementary information file).

2. The interaction of berberine with hydrated amines

2.1. Primary amines

The crystal structure of berberine (**1**) is relatively complicated. According to X-ray structural analysis, its unit cell contains the organic cation, chloride anion, and four molecules of water that are linked by hydrogen bonds (Fig. 4).[18]

The structures of its 9-amino derivatives **4** are at least as complex. For example, according to the data of X-ray structural study, compound **4a** formed a chloride salt crystal solvate with unit cell containing two independent molecules **4a**, as well as water and nitrobenzene in 2:3:1 ratio (Fig. 5). The presence of several proton donor and acceptor groups in compound **4a** created a strong hydrogen bond network. Thus, the crystal contained hydrated chloride ion chains, featuring an alternating sequence of six-membered $(H_2O)_4Cl_2$ and four-membered $(H_2O)_2Cl_2$ rings. The Cl···H–O and O···H–O distances characterizing the strength of hydrogen bonds in the aforementioned chains were 2.306(4)–2.334(4) Å and 2.002 (2) Å, respectively. The water molecules involved in the four-membered rings also formed hydrogen bonds with the amino groups of cations, with the N–H···O distances ranging from 2.104 to 2.192 Å.

The obtained experimental and computational data clearly indicate that the presence of crystal hydrate water in the reaction media had an important effect on the structure of the starting berberine (**1**) and its amination products **4**. For this reason, in the next step we calculated the MEP for berberine reaction with hydrated methylamine and dimethylamine. The first calculation was performed for a direct attack by methylamine hydrate (**8**) on berberine, where the water molecule acts as a bifunctional catalyst for the process (Scheme 5).

The process commences by a barrierless formation of the initial complex **9**, in which a water molecule is linked by a hydrogen bond to the oxygen atom of methoxy group at the C-10 atom, while the amine molecule donates a proton forming a hydrogen bond with a water molecule. The complex **9** is more stable by 0.8 kcal/mol than the reactants at infinite separation.

The complex **9** was further transformed over a 10.8 kcal/mol energy barrier to the Meisenheimer complex **10'**, in which 1,3-sigmatropic migration of hydroxonium ion (proton

Scheme 4

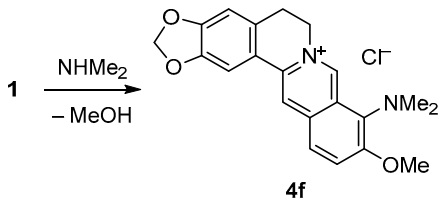

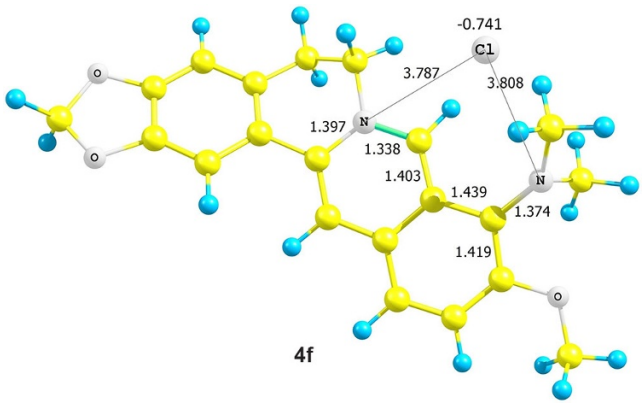

Figure 3. The calculated interatomic distances (Å) in 9-*N*,*N*-dimethylberberine (**4f**). The Mulliken charge on the chloride ion is also shown.

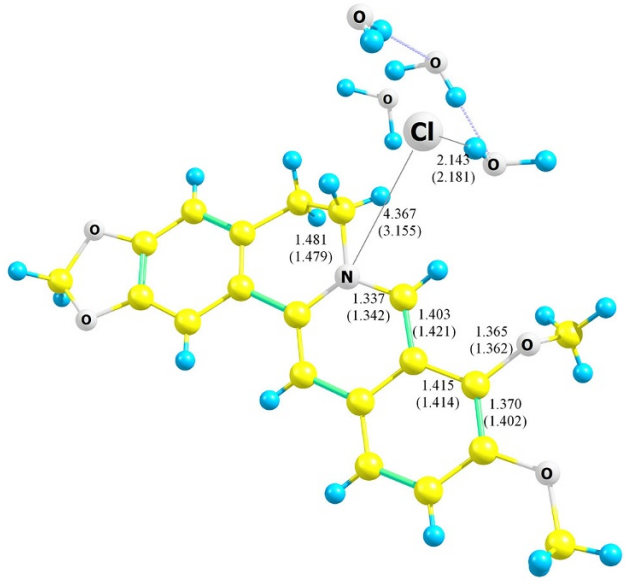

Figure 4. The crystal structure of berberine according to X-ray structural analysis data.[18] The results of our DFT calculations are shown in parentheses. The interatomic distances are given in Å.

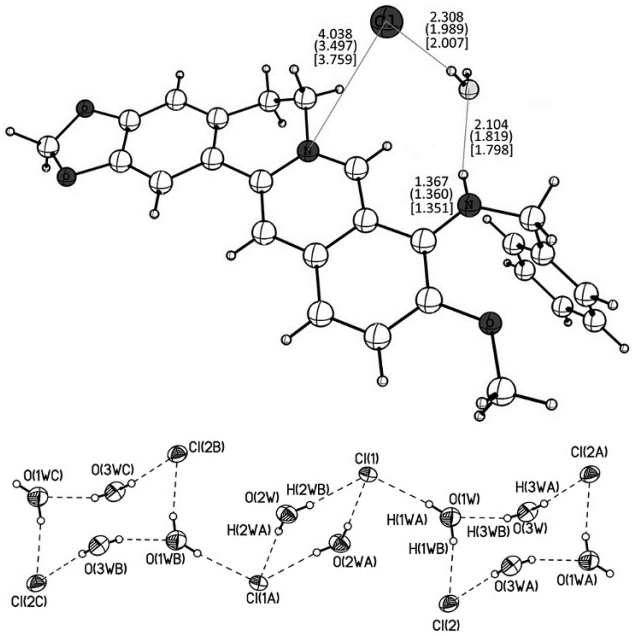

Figure 5. Top: the main geometrical characteristics of 9-*N*-benzylberberine (**4a**) according to X-ray structural analysis. The calculated values are given in round parentheses. The values obtained by quantum-chemical calculations for 9-*N*-methyl-berberine monohydrate (**4e**) are given in square parentheses. The interatomic distances are given in Å. Bottom: hydrated chloride chains in the crystal of 9-*N*-benzylberberine (**4a**) according to X-ray structural analysis.

transfer by a water molecule from amino group to the metoxy group) led to the formation of complex **10''** (Fig. 6, Table S4 in the Supplementary information file). A plateau on MEP with energy barriers not exceeding 1–2 kcal/mol corresponded to the proton transfer. It should be noted that one of the hydrogen atoms in the water molecule was linked by a stabilizing interaction to the chloride ion during all process stages. The complex **11**, consisting of *N*-methyl-berberine, a methanol molecule, water, and chloride ion linked by hydrogen bonds was formed during the amination reaction. The formation of complex **11** was thermodynamically favorable by 17.5 kcal/mol relative to the pre-reaction complex **9**.

We further considered another sequence of events: an initial attack by water molecule producing the complex of berberrubine **14** and only then an attack by amine, resulting in *N*-methylberberine **16** (Scheme 6). In this case, the calculations indicated that the interaction of berberine with hydrated methylamine **8** occurs strictly stepwise. The reaction proceeds with the formation of complex **12**, in which a water molecule is linked to methylamine, and the water molecule donates a proton for the hydrogen bond, in contrast to the complex **9**. The complex **12** is more stable by 10.1 kcal/mol than the reactants at infinite separation.

In the first step, where the activation energy barrier of **TS 5** is equal to 17.9 kcal/mol, a water molecule attacks berberine at position C-9, forming a Meisenheimer complex (structure **13'**, MEP minimum, Fig. 6). After that, a 1,3-sigmatropic migration of methylammonium (proton transfer) from the oxygen atom of water molecule to the oxygen atom of metoxy group occurs in the second step. It should be noted that this transformation is practically barrierless, and the energy difference of intermediate structures and isomers **13'** and **13''** is quite insignificant – within the limits of 1–2 kcal/mol (the MEP plateau, Fig. 6). In the third step of the process, **TS 6** is reached with merely 2.6 kcal/mol energy and the thermodynamically stable system **14** is formed, representing a complex of three molecules, methylamine, methanol, and berberrubine.

Remarkably, in the first three stages of the process presented in Scheme 6, the molecule of methylamine always participates in a N···H···O hydrogen bridge, with only slight structural changes. During the 1,3-sigmatropic shift, the length of O···H bond also changes only slightly from the structure **12** to berberrubine complex **14** (from 1.790 to 1.768 Å according to DFT calculations), despite the significant size of the migrating ammonium ion, correlating with the small activation energy at this stage. In order to better understand the role of methylamine in the formation of berberrubine (**3**) (**12**→**14**), we modeled the reaction of berberine (**1**) with water dimer – isoelectronic analog of methylamine hydrate (**8**) (Scheme 7).

An earlier experimental study showed that the hydrolysis of berberine leads to the formation of berberrubine (**3**), when this process occurs under extreme

Scheme 5

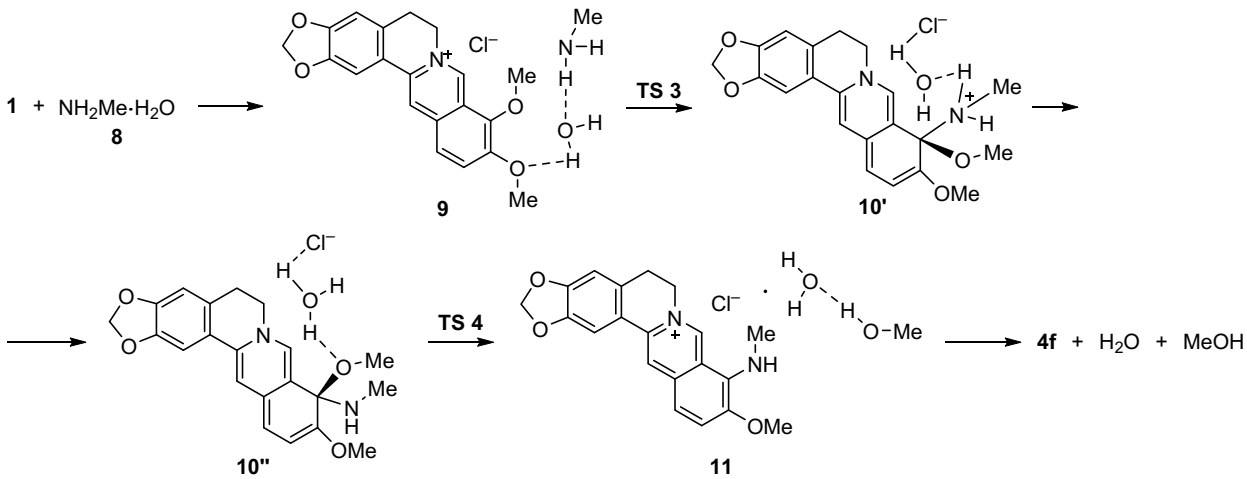

Scheme 6

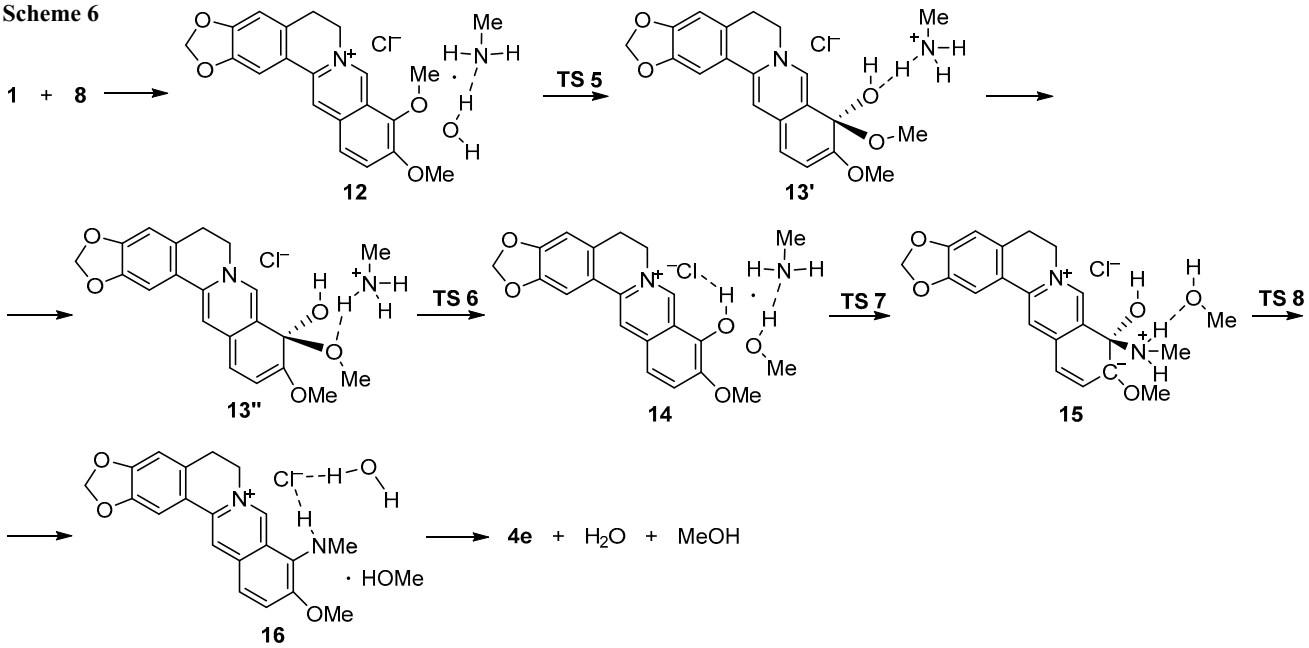

conditions – high temperatures and low pressure (Scheme 1).[19] Indeed, according to our calculations, the MEP of such process first involves the formation of complex **17**, stabilized by 24.6 kcal/mol relative to infinitely separated reactants, and proceeds through three higher energy transition states. The first of these transition states (**TS 9**) is rate limiting – the energy barrier of this stage is maximal, equal to 33.0 kcal/mol (Table S5 in the Supplementary information file).

The kinetically and thermodynamically unstable σ-complex **18'** was formed in the first step. The complex **18'** underwent further transformations through intermediate stationary points with insignificant energy differences, involving the transfer of second (distant) water molecule from the arriving OH group to the leaving metoxy group (formation of complex **18''**, the plateau in Figure 7). In this sense, the sequence of steps in the hydrolysis of berberine (**1**) by water dimer was not principally different from the hydrolysis of berberine (**1**) by methylamine hydrate (**8**). According to calculations, the O···H bond length in the hydrogen bridge also changed only insignificantly from 1.888 to 1.762 Å, when going from the structure **17** to structure **19** *via* the transition state **TS 10**. The final product, as expected, was the complex of berberrubine with hydrated methanol **19**.

It should also be noted that the relative values of energy barriers limiting the first stages of berberine hydrolysis with water dimer and methylamine hydrate (Figs. 6, 7)

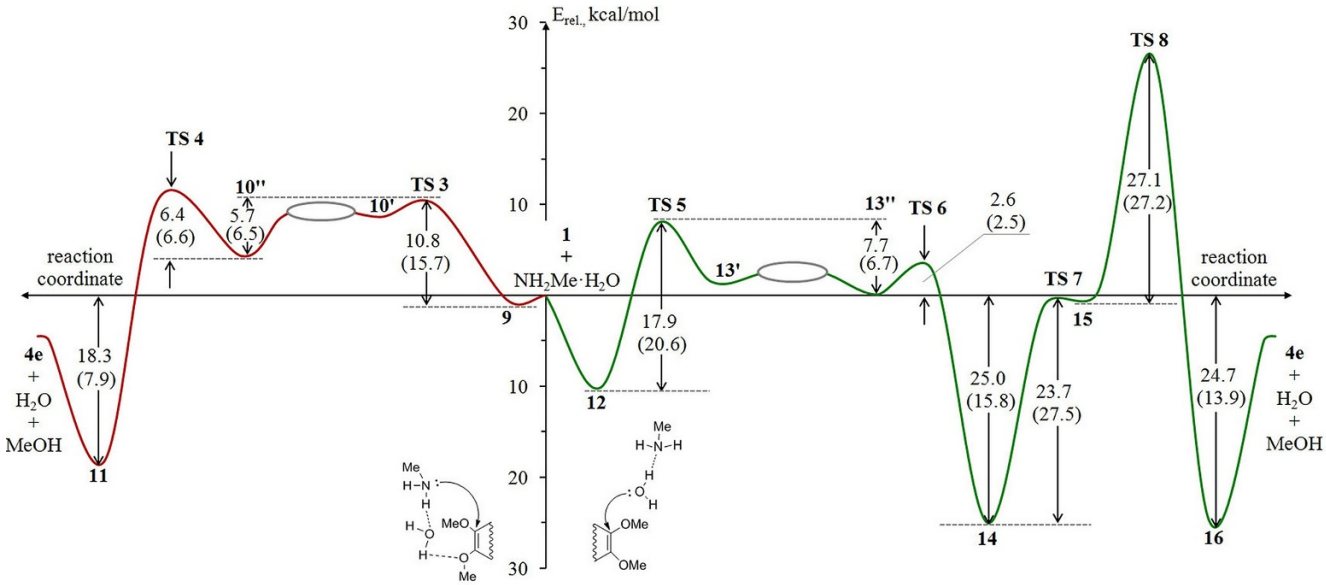

Figure 6. MEP of berberine (**1**) amination with methylamine hydrate (**8**) through the stage of complex **14** (right side) and direct amination (left side). The relative energy values include corrections for ZPE. The relative Gibbs free energy values are given in parentheses. The total energy of isolated reactants is assumed as reference.

Scheme 7

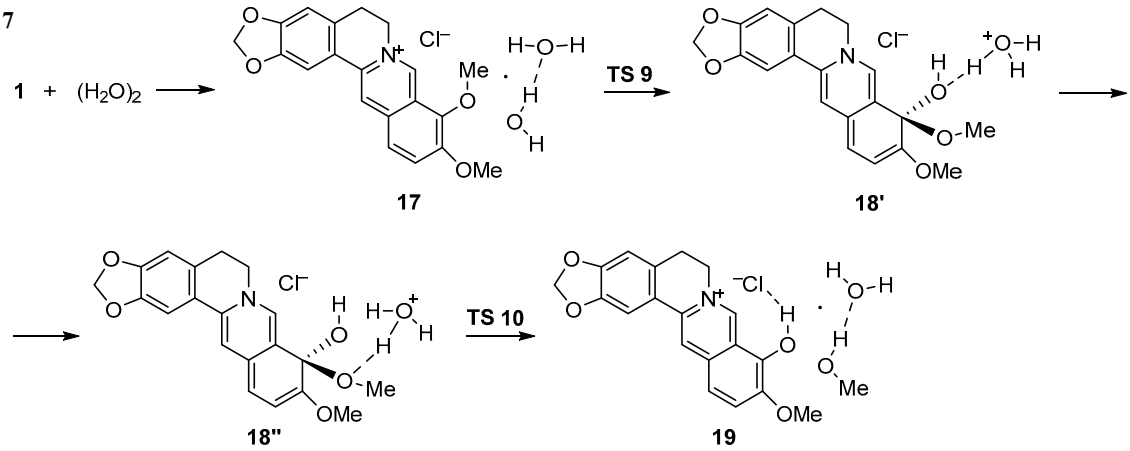

correlated with the Parr's global electrophilicity indices, calculated by a known method for both reactants.[21] As expected, the value of ω for the complex **8** was 0.37 eV, while for the dimer $(H_2O)_2$ it was 0.56 eV, indicating a decrease of nucleophilicity when changing from methylamine hydrate to dimer of water.

In aqueous medium this process can lead to two isomeric complexes **8** and **8'**. Obviously, the tricoordinated nitrogen atom in complex **8** causes amination of berberine, while the dicoordinated oxygen atom in complex **8'** is responsible for berberine hydrolysis at position C-9 (Fig. 8).

Even though the hydrolysis by dimer of water is obviously thermodynamically favorable (the energy effect is equal to 9.9 kcal/mol), practically it can be achieved only under forcing conditions, according to the published experimental procedures. Additionally, this provides an insight into the role of methylamine molecule in the transformation of berberine (**1**) to berberrubine (**3**): methylamine apparently acts as a bifunctional catalyst, facilitating the first (rate limiting) step of the process.

Returning to Scheme 6, we should note an important feature of berberine reaction with methylamine hydrate, in that the further amination of berberrubine (**3**) according to the route **14→15→16** must occur under more forcing conditions, compared to the first three steps. Indeed, calculations showed that the transformation **14→15** proceeds with a high energy barrier of **TS 7** equal to 23.7 kcal/mol (Fig. 6), and the complex **15** thus obtained must cross another significant energy barrier of **TS 8** (27.1 kcal/mol) in order to achieve aromatization.

The formation of amino derivative **16** from the berberrubine complex **14** is slightly unfavorable energetically by merely 0.3 kcal/mol. Additional *ab initio* (RHF/6-31G**) computational analysis of the stationary points **14** and **16** showed that the final reaction product **16** is more stable than the hydrolysis product **14** by 0.8 kcal/mol. It should be pointed out that the methanol molecule in complex **16** was not linked by hydrogen bonds to other structures. Despite the total favorable energy effect of 14.6 kcal/mol relative to the starting system **12**, the process with kinetic control of steps **14→15→16** can not produce compounds **4a–d** under relatively mild conditions.

Thus, if follows from the results of quantum-chemical calculations that the reaction with methylamine requires

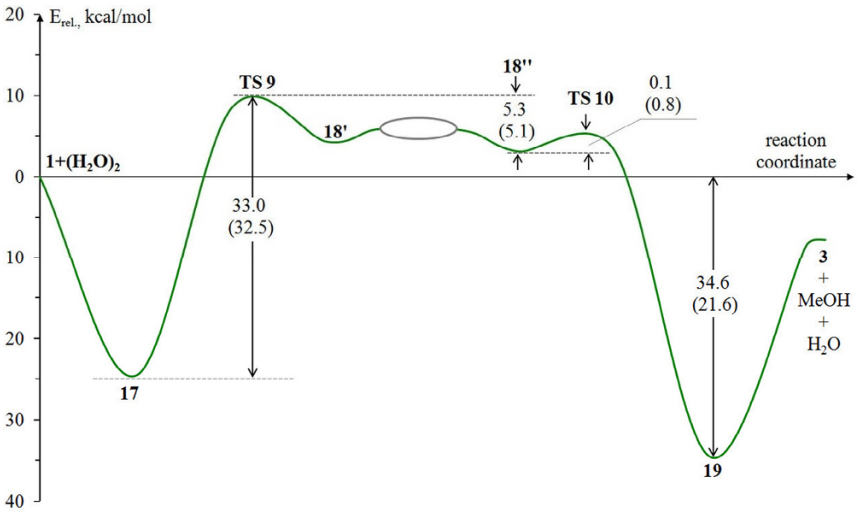

Figure 7. MEP of berberine hydrolysis with a dimer of water. The relative energy values include corrections for ZPE. The relative Gibbs free energy values are given in parentheses. The total energy of isolated reactants is assumed as reference.

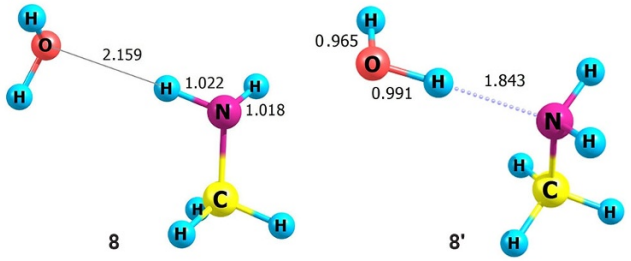

Figure 8. The structures of methylamine–water clusters (**8**) according to B3LYP/6-31G** calculations. The most important interatomic distances are in Å.

less energy and leads directly to 9-amino derivatives of berberine. The presence of crystal hydrate water in the starting berberine (**1**) facilitates its direct amination, but can lead to the formation of hydrolysis product – berberrubine (**3**) in small amounts.

2.1. Secondary amines

We also investigated experimentally the interaction of berberine with secondary aliphatic amines: piperidine, morpholine, piperazine, *N*-piperonylpiperazine, and homopiperazine. The reactions were continued for 1–24 h at reflux conditions in anhydrous solvents: ethanol, butanol, and acetonitrile. The reactions with anhydrous piperidine and morpholine were also performed without solvent at the reflux temperatures of amines. In none of the cases we were able to detect the formation and to isolate the respective 9-*N*-dialkyl derivatives of berberine from the reaction mixtures. It was found that the reaction of berberine with secondary amines gave 23–82% yields of berberine hydrolysis product – berberrubine (**3**) in each experiment (Scheme 1).

Since the observed hydrolysis in anhydrous media can be explained only by the presence of crystal hydrate water in berberine itself, we prepared completely anhydrous berberine by heating berberine hydrate under vacuum in the presence of P_2O_5.[22] No hydrolysis was observed upon interaction of dehydrated berberine free of crystal hydrate water with secondary amines in anhydrous alcohols, as the reaction mixture contained only unchanged reagents. At the same time, the formation of berberrubine (**3**) occurred after the addition of even catalytic amounts (0.2 equiv) of secondary amine.

The simplest model selected by us for the quantum-chemical study of berberine amination with secondary amines was the process involving berberine complex with dimethylamine hydrate (Scheme 8).

The amination of berberine (**1**) with dimethylamine proceeded through the thermodynamically favored complex **20**, more stable by 10.5 kcal/mol than the reactants at infinite separation, in which the dimethylamine molecule participated in an N···H···Cl hydrogen bond. However, the initial attack by amine at the C-9 atom was not thermodynamically favored, since the postreaction complex **21** was less stable by 11.5 kcal/mol than the reactants (Table S6 in the Supplementary information file). The latter fact can be explained by the absence of stabilizing (attractive) interactions in the product **21** between the chloride ion and hydroxyl group protons (Fig. S10 in the Supplementary information file). Besides that, the water and methanol molecules in complex **21** are not far removed from the reaction site. The water molecule in this case is linked by a bridging proton to the dimethylamino group, while the methanol molecule in complex **21** is not linked to the rest of the system by hydrogen bonds according to AIM calculations.

The conclusions are entirely different when the sequence of reaction steps is changed – berberine (**1**) is first attacked by water, then by dimethylamine (Scheme 9).

Thus, according to calculations, the first two steps of berberine (**1**) hydrolysis by dimethylamine hydrate (Scheme 9) are analogous to those of berberine (**1**) reaction with methylamine hydrate (**8**) (Scheme 6). Initially the complex **22** is formed, which is more stable by 9.9 kcal/mol than the isolated reactants (Fig. 9). Then the position C-9 is attacked by dimethylamine hydrate, leading to the formation of thermodynamically stable complex **23'**. This particular step is rate limiting for the whole process, with the energy barrier of **TS 11** equal to 16.6 kcal/mol (Fig. 9, Table S7 in the Supplementary information file).

This step is followed by 1,3-sigmatropic shift of dimethylammonium ion from one oxygen atom to the other (**23'→23''**). Such a stepwise migration is reflected, similarly to the earlier example, by a plateau on MEP, where the energy changes due to local minima and conformational barriers do not exceed 2–3 kcal/mol. The reaction site of the molecule does not significantly rearrange during these steps (Fig. 9).

In the third step, an associate of methanol and dimethylamine molecules leave the complex **23''**, taking only 3.0 kcal/mol of energy (transition state **TS 12**). The obtained product **24** is significantly (by 25.5 kcal/mol) more stable than the the starting system of infinitely separated reactants.

It was shown experimentally and by quantum-chemical calculations that direct amination at the C-9 position of berberine is preferred in the case of primary amines, instead of hydrolysis to berberrubine followed by its amination. The amination reaction with dimethylamine in the presence

Scheme 8

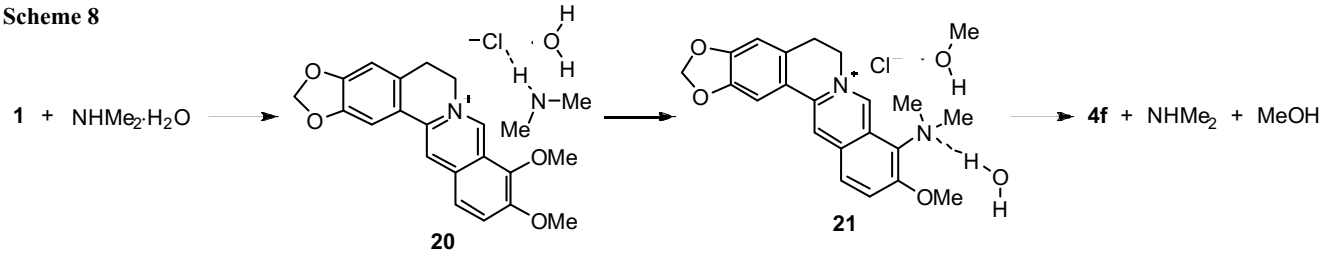

Scheme 9

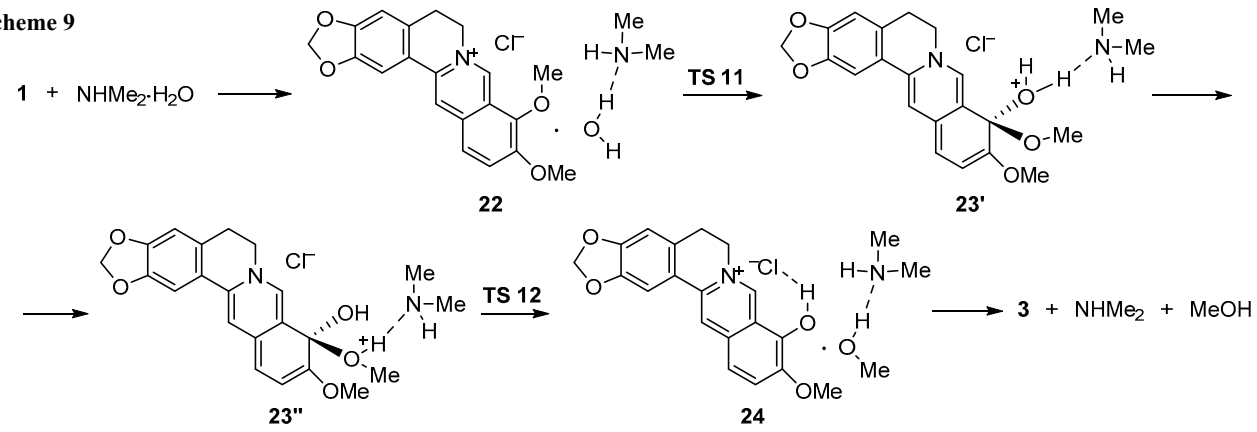

of crystal hydrate water proceeds as a stepwise hydrolysis of the O–Me bond at the C-9 atom, with the eventual formation of berberrubine. Direct amination at the same atom does not occur for energy reasons. In order to explain why the reaction is more facile in the case of attack by methylamine hydrate at the C-9 atom of berberine, we compared the local nucleophilicity indices ω_k^- of the nitrogen atoms. According to calculations, the ω_k^-(N) index in the amination reaction increased from 0.18 to 0.32 eV when going from methylamine to its monohydrate.

The same effect was observed also when comparing isolated dimethylamine and its hydrate: ω_k^-(N) for the reaction of berberine amination increased from 0.14 to 0.26 eV. However, the determining factor in choosing the mechanism of nucleophilic attack at the C(9) atom – either amination or hydrolysis, was the thermodynamics of the process. In the case of amination, the reaction thermodynamics were obviously unfavorable, and hydrolysis occurred at the reaction site. Besides that, we can conclude that the driving force of all aforementioned reactions is the stabilization of product due to the formation of hydrogen bonds.

The results of this work showed that the methods for synthesis of berberine 9-dialkylamino derivatives, analogous to those developed for monoalkylamino derivatives, are not feasible and the search for new synthetic approaches is necessary. One of the options is changing the anion and including the target molecule in solvate cage or in a suitable complex.

Based on this study, a completely new approach can be proposed for the preparation of berberine 9-hydroxy derivatives, using much milder conditions than the previously described reactions and giving higher yields, thus it is particularly applicable to the hydrolysis of less stable derivatives of berberine.

Experimental

^{1}H and ^{13}C NMR spectra were acquired on a Bruker DPX-250 spectrometer (250 and 63 MHz, respectively) in DMSO-d_6, internal standard TMS. ^{1}H NMR signals were assigned by using two-dimensional COSY and NOESY spectroscopy data (mixing time 0.6–1.3 s). Several of the ^{13}C NMR signals overlapped, thus the observed number of signals was smaller than expected theoretically. High-

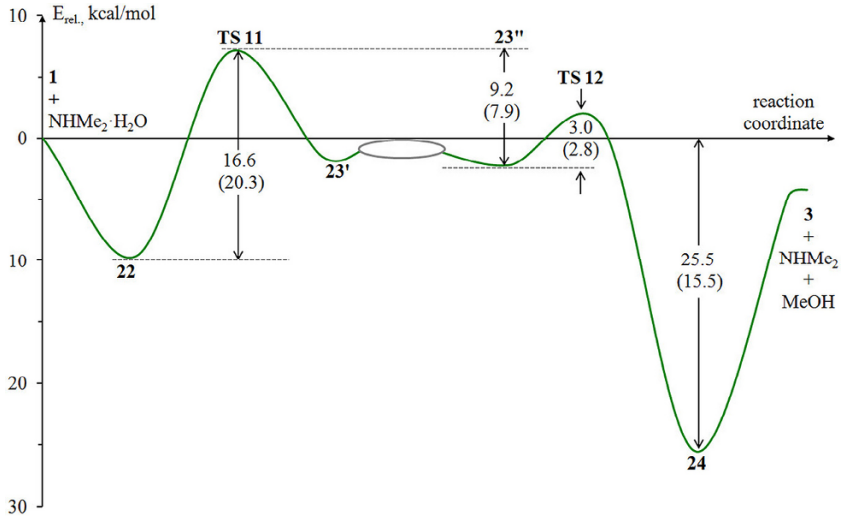

Figure 9. MEP of nucleophilic attack by dimethylamine hydrate on berberine (**1**). The relative energy values include corrections for ZPE. The relative Gibbs free energy values are given in parentheses. The total energy of isolated reactants is assumed as reference.

resolution mass spectra were recorded on a Bruker micrOTOF II instrument, with electrospray ionization. The measurements were performed in positive ion mode (capillary voltage 4500 V), the mass scanning range was 50–3000 Da. Melting points were determined in glass capillaries on a PTP apparatus. Merck Silicagel 60 (70–230 μm) was used for column chromatography. Commercially available berberine chloride hydrate, tryptamine, serotonin, piperazine, homopiperazine, morpholine, piperonylpiperazine (Alfa Aesar), benzylamine (Lancaster Synthesis), and furfurylamine (Acros Organics) were used for the syntheses.

Computational methodology. Gas phase quantum-chemical calculations were performed by density functional theory (DFT) using 6-31G** basis set and B3LYP functional, including the Becke three-parameter exchange functional[23,24] and the Lee–Young–Parr correlation functional.[25] The selection of a basis set that is widely applied to the study of processes involving nucleophilic attack[26–28] was justified by the complexity of alkaloids, as well as the reaction mechanisms. When needed, *ab initio* calculations were also performed with the same basis set.

Complete geometry optimization for the structures corresponding to stationary points on MEP was continued until the gradient value reached 10^{-7} hartree/bohr, using Gaussian 03 software suite[29] running on a Silver cluster at the Chemistry Department of the Southern Federal University.

The nature of stationary points was established by calculation of the normal vibrational frequencies (Hesse matrices).[30] The MEP of reactions were found by following the gradient from transition states in the direct and reverse directions of the reaction coordinate.[31] The analysis of electron density distribution function according to the AIM model was performed according to a published method.[17]

Synthesis of berberrubine chloride (3). Secondary amine (3.0 mmol) was added to a solution of berberine chloride (**1**) (372 mg, 1.0 mmol) in ethanol (25 ml). The mixture was refluxed for 4–5 h, then ethanol was removed by distillation. The residue was separated by chromatography on silica gel (eluent 10:1 $CHCl_3$–EtOH), collecting the fraction with R_f 0.40, which was then recrystallized from THF or acetone. Yield 65–82%, red needles, decomp. 279–282°C (decomp. 270–285°C[19]). The obtained berberrubine chloride was identical to a sample reported in the literature.[19]

Synthesis of 9-*N*-substituted berberine derivatives 4a–d (General method). The appropriate amine (5.0 mmol) was added to berberine chloride (372 mg, 1.0 mmol), the mixture was heated for 4–5 h at 120°C, the reaction mixture was washed with acetone (3×10 ml) to remove the remaining amine. The dry residue was separated by chromatography on silica gel (eluent 10:1 $CHCl_3$–EtOH), the obtained compounds were recrystallized from acetone or THF.

***N*-Benzylberberine chloride (4a)** matched a sample reported in the literature.[8] Yield 289 mg (65%).

***N*-(Furan-2-ylmethyl)berberine chloride (4b)**. Yield 240 mg (58%), red needles, mp 270–272°C (THF). ^{1}H NMR spectrum, δ, ppm (*J*, Hz): 3.15–3.19 (2H, m, 5-CH_2); 3.95 (3H, s, 10-OCH_3); 4.70–4.78 (4H, m, 6-CH_2, NCH_2); 6.16 (2H, s, OCH_2O); 6.19 (1H, d, *J* = 2.8, H-3'); 6.29 (1H, dd, *J* = 2.8, *J* = 2.5, H-4'); 6.76 (1H, br. s, NH); 7.08 (1H, s, H-4); 7.53–7.58 (2H, m, H-12, H-5'); 7.77 (1H, s, H-1); 7.94 (1H, d, *J* = 8.8, H-11); 8.74 (1H, s, H-13); 10.09 (1H, s, H-8). ^{13}C NMR spectrum, δ, ppm: 27.0; 44.0; 55.5; 57.3; 102.5; 106.7; 107.7; 108.9; 110.8; 118.3; 120.3; 121.0; 125.3; 130.7; 133.5; 136.0; 136.4; 142.7; 146.5; 148.1; 150.0; 135.9. Found, *m*/*z*: 401.1486 $[M–Cl]^+$. $C_{24}H_{21}N_2O_4$. Calculated, *m*/*z*: 401.1496.

***N*-[2-(1*H*-Indol-3-yl)ethyl]berberine chloride (4c)**. Yield 298 mg (60%), red needles, mp 279–280°C (acetone). ^{1}H NMR spectrum, δ, ppm (*J*, Hz): 3.05 (2H, t, *J* = 5.0, $NC\underline{H_2}CH_2$); 3.18–3.22 (2H, m, 5-CH_2); 3.89–3.94 (2H, m, $NCH_2C\underline{H_2}$); 3.96 (3H, s, OCH_3); 4.70–4.76 (2H, m, 6-CH_2); 6.18 (2H, s, OCH_2O); 6.48 (1H, m, 9-NH); 6.96 (1H, t, *J* = 7.4, H-5'); 7.03–7.06 (1H, m, H-6'); 7.09 (1H, s, H-2'); 7.20 (1H, s, H-4); 7.35 (1H, d, *J* = 7.9, H-7'); 7.47–7.54 (2H, m, H-12, H-4'); 7.77 (1H, s, H-1); 7.88 (1H, d, *J* = 8.7, H-11); 8.68 (1H, s, H-13); 9.95 (1H, s, H-8); 10.92 (1H, s, 1'-NH). ^{13}C NMR spectrum, δ, ppm: 24.5; 27.8; 53.1; 56.3; 102.1; 102.6; 105.2; 108.8; 110.5; 112.0; 117.9; 118.6; 118.8; 120.3; 121.5; 122.2; 123.7; 127.4; 129.8; 132.5; 133.9; 136.8; 146.6; 147.8; 148.9; 149.9; 166.3. Found, *m*/*z*: 464.1966 $[M–Cl]^+$. $C_{29}H_{26}N_3O_3$ Calculated, *m*/*z*: 464.1969.

***N*-[2-(5-Hydroxy-1*H*-indol-3-yl)ethyl]berberine chloride (4d)**. Yield 288 mg (56%), red needles, decomp. 256–258°C (THF). ^{1}H NMR spectrum, δ, ppm (*J*, Hz): 2.94–3.05 (6H, m, $N(CH_2)_2$, 5-CH_2); 3.75 (3H, s, 10-OCH_3); 4.50–4.54 (2H, m, 6-CH_2); 6.09 (2H, s, OCH_2O); 6.52 (1H, d, *J* = 7.9, H-12); 6.60–6.64 (2H, m, H-6', 9-NH); 6.83 (1H, s, H-2'); 6.97 (1H, s, H-4); 7.11 (1H, s, H-4'); 7.14 (1H, d, *J* = 8.8, H-7'); 7.32 (1H, d, *J* = 7.9, H-11); 7.63 (1H, s, H-1); 8.09 (1H, s, H-13); 8.76 (1H, br. s, OH); 9.16 (1H, s, H-8); 10.68 (1H, s, 1'-NH). ^{13}C NMR spectrum, δ, ppm: 23.7; 27.8; 39.7; 53.3; 102.1; 102.5; 105.2; 108.8; 109.0; 112.0; 112.3; 118.0; 120.1; 121.8; 122.2; 124.1; 128.0; 129.9; 131.3; 132.4; 134.0; 146.5; 147.8; 148.9; 149.7; 150.8 Found, *m*/*z*: $[M–Cl]^+$ $C_{29}H_{26}N_3O_4^+$. Calculated, *m*/*z*: 480.1918.

X-Ray structural study of compound 4a. Crystals suitable for X-ray structural analysis were obtained by slow evaporation of a nitrobenzene solution of compound **4a**. The composition of the colorless crystals was $C_{26}H_{23}ClN_2O_3 \cdot 0.5C_6H_5NO_2 \cdot 1.5H_2O$ (*M* 535.49). The X-ray structural study was performed on an automated Bruker APEX II diffractometer (graphite monochromator, λ(MoKα) 0.71073 Å, ω-scanning) at 120 K. Empirical accounting for absorption and the correction of systematic errors were performed with the SADABS software. The structure was solved by a direct method and refined by full matrix method of least squares by F^2_{hkl} with anisotropic thermal parameters for all non-hydrogen atoms. The positions of hydrogen atoms in amino groups and water molecules were revealed by differential Fourier synthesis, the hydrogen positions at the carbon atoms were calculated. The solving and refinement of structure were performed with the SHELX 2009-9.13 software suite.[32] The complete

crystallographic dataset was deposited at the Cambridge Crystallographic Data Center[33] (deposit CCDC 1421105).

The Supplementary information file containing the geometrical characteristics of structures **5**–**24** and the transition states, as well as the full and relative energy (in tabular form) for all stationary points on the reaction MEP is available online at http://link.springer.com/journal/10593.

This work was performed within the framework of Project part of the State Assignment No.4.129.2014/K from the Ministry of Education and Science of the Russian Federation.

References

1. Saha, S. K.; Khuda-Bukhsh, A. R. *Eur. J. Pharmacol*. **2013**, *714*, 239.
2. Siow, Y. L; Sarna, L; Karmin, O. *Food Res. Int*. **2011**, *44*, 2409.
3. Khazir, J.; Mir, B. A.; Pilcher, D. L.; Riley, D. L. *Phytochem. Lett.* **2004**, *7*, 173.
4. Crycova, L.; Dostal, J.; Marek, R. *Phytochem.* **2007**, *68*, 150.
5. Ji, H.-F.; Shen, L. *Molecules* **2011**, *16*, 6732.
6. Krivogorsky, B.; Pernat, J. A.; Douglas, K. A.; Czerniecki, N. J.; Grundt, P. *Bioorg. Med. Chem. Lett.* **2012**, *22*, 2980.
7. Nechepurenko, I. V.; Salakhutdinov, N. F.; Tolstikov, G. A. *Khimiya v Interesakh Ustoichovogo Razvitiya* **2010**, *18*, 1.
8. Shan, W.-J.; Huang, L.; Zhou, Q.; Meng, F.-Ch.; Li, X.-Sh. *Eur. J. Med. Chem*. **2011**, *46*, 5885.
9. Huang, L.; Shi, A.; He, F.; Li, X. *Bioorgan. Med. Chem*. **2010**, 18, 1244.
10. Ma, Y.; Ou, T.-M.; Hou, J.-Q.; Lu, Y.-J.; Tan, J.-H.; Gu, L.-Q.; Huang, Zh.-Sh. *Bioorg. Med. Chem*. **2008**, *16*, 7582.
11. Ma, Y.; Ou, T.-M.; Tan, J.-H.; Hou, J.-Q.; Huang, Sh.-L.; Gu, L.-Q.; Huang, Zh.-Sh. *Eur. J. Med. Chem.* **2011**, *46*, 1906.
12. Huang, L.; Luo, Z.; He, F.; Shi, A. *Bioorg. Med Chem. Let*. **2010**, *20*, 6649.
13. Ma, Y.; Ou, T.-M.; Tan, J.-H.; Hou, J.-Q.; Huang, Sh.-L. *Bioorg. Med. Chem. Let*. **2009**, *19*, 3414.
14. Bodiwala, H. S.; Sabde, S.; Mitra, D.; Bhutani, K. K.; Singh, I. P. *Eur. J. Med. Chem*. **2011**, *46*, 1045.
15. Burov, O. N.; Kurbatov, S. V.; Morozov, P. G.; Kletskii, M. E.; Tatarov, A. V. *Chem. Heterocycl. Compd.* **2015**, *51*, 772. [*Khim. Geterotsikl. Soedin.* **2015**, *51*, 772.]
16. Lam, Y. *Int. J. Pharma Sci. Res.* **2014**, *5*, 350.
17. Bader, R. F. W. *Atoms in Molecules. Quantum Theory* [Russian translation]; Mir, Moscow, 2001.
18. Kariuki, B. M.; Jones, W. *Acta Cryst. Sect. C* **1995**, *51*, 1234.
19. Iwasa, K.; Kamigauchi, M.; Uek, M.; Taniguch, M. *Eur. J. Med. Chem.* **1996**, *31*, 469.
20. Gorb, L.; Podolyan, E.; Dziekonski, P.; Sokalski, W. A.; Leszczynski, J. *J. Am. Chem. Soc*. **2004**, *126*, 10119.
21. Jovené, C.; Jacquet, M.; Marrot, J.; Bourdreux, F.; Kletsky, M. E.; Burov, O. N.; Gonçalves, A.-M.; Goumont, F. *Eur. J. Org. Chem.* **2014**, 6451.
22. Elliott, I. W. *J. Heterocycl. Chem*. **1967**, *4*, 639.
23. Becke, A. D. *Phys. Rev. A*. **1988**, 38, 3098.
24. Becke, A. D. *J. Chem. Phys*. **1993**, 98, 5648.
25. Lee, C.; Yang, W.; Parr, R. G. *Phys. Rev. B*. **1988**, *37*, 785.
26. Burov, O. N.; Kletskii, M. E.; Gulevskaya, A. V. *Russ. Chem. Bull*. **2013**, *62*, 1156. [*Izv. Akad. Nauk*, *Ser. Khim.* **2013**, 1155.]
27. Kletskii, M. E.; Burov, O. N.; Dalinger, I. L.; Shevelev, S. A. *Comp. Theor. Chem*. **2014**, *1033*, 31.
28. Suzdalev, K. F.; Den'kina, S. V.; Starikova, A. A.; Dvurechensky, V. V.; Kletsky, M. E.; Burov, O. N. *Mendeleev Commun.* **2011**, *21*, 231.
29. Frisch, M. J.; Trucks, G. W.; Schlegel, H. B.; Scuseria, G. E.; Robb, M. A.; Cheeseman, J. R.; Montgomery, J. A.; Vreven, Jr. T.; Kudin, K. N.; Burant, J. C.; Millam, J. M.; Iyengar, S. S.; Tomasi, J.; Barone, V.; Mennucci, B.; Cossi, M.; Scalmani, G.; Rega, N.; Petersson, G. A.; Nakatsuji, H.; Hada, M.; Ehara, M.; Toyota, K.; Fukuda, R.; Hasegawa, J.; Ishida, M.; Nakajima, T.; Honda, Y.; Kitao, O.; Nakai, H.; Klene, M.; Li, X.; Knox, J. E., Hratchian, H. P.; Cross, J. B.; Bakken, V.; Adamo, C.; Jaramillo, J.; Gomperts, R.; Stratmann, R. E.; Yazyev, O.; Austin, A. J.; Cammi, R.; Pomelli, C.; Ochterski, J. W.; Ayala, P. Y.; Morokuma, K.; Voth, G. A.; Salvador, P.; Dannenberg, J. J.; Zakrzewski, V. G.; Dapprich, S.; Daniels, A. D.; Strain, M. C.; Farkas, O.; Malick, D. K.; Rabuck, A. D.; Raghavachari, K.; Foresman, J. B.; Ortiz, J. V.; Cui, Q.; Baboul, A. G.; Clifford, S.; Cioslowski, J.; Stefanov, B. B.; Liu, G.; Liashenko, A.; Piskorz, P.; Komaromi, I.; Martin, R. L.; Fox, J. D.; Keith, T.; Al-Laham, M. A.; Peng, C. Y.; Nanayakkara, A.; Challacombe, M.; Gill, P. M. W.; Johnson, B.; Chen, W.; Wong, M. W.; Gonzalez, C.; Pople, J. A. *Gaussian 03*; Gaussian, Inc.: Wallingford, 2004.
30. Schlegel, H. B. *Theor. Chim. Acta* **1984**, *66*, 333.
31. Hirsh, M.; Quapp, W. *Chem. Phys. Lett*. **2004**, *395*, 150.
32. Sheldrick, G. M. *Acta Crystallogr*., *Sect. A: Found. Crystallogr.* **2008**, *A64*, 112.
33. Allen, F. H. *Acta Crystallogr*., *Sect. B: Struct. Sci.* **2002**, *B58*, 380.